# Characterization of nickel sulfate supported on $SiO_2$–$Al_2O_3$ for ethylene dimerization and its relationship to acidic properties

Jong Rack Sohn[a,*], Won Cheon Park[a], and Sang-Eon Park[b]

[a] *Department of Industrial Chemistry, Engineering College, Kyungpook National University, Taegu 702-701, Korea*
[b] *Korea Research Institute of Chemical Technology, Taejon 305-606, Korea*

Received 17 January 2002; accepted 21 March 2002

A series of catalysts, $NiSO_4/SiO_2$–$Al_2O_3$, for ethylene dimerization were prepared by the impregnation method using aqueous solution of nickel sulfate. Although $SiO_2$–$Al_2O_3$ without $NiSO_4$ was inactive as catalyst for ethylene dimerization, the $SiO_2$–$Al_2O_3$ with $NiSO_4$ exhibited high catalytic activity even at room temperature. The high catalytic activity of $NiSO_4/SiO_2$–$Al_2O_3$ was closely correlated with the increase of acidity and acid strength due to the addition of $NiSO_4$. The sample having 15 wt% of $NiSO_4$ and calcined at 500 °C for 1.5 h exhibited maxima for catalytic activity and acidity. In view of IR results of CO adsorbed on $NiSO_4/SiO_2$–$Al_2O_3$, it is concluded that the active sites responsible for ethylene dimerization consist of a low-valent nickel, $Ni^+$, and an acid.

**KEY WORDS:** ethylene dimerization; nickel sulfate on silica–alumina; acidity; acid strength; active site.

## 1. Introduction

The dimerization of alkenes is an important method for the production of higher olefins which find extensive application as industrial intermediates. A considerable number of papers have dealt with the problem of nickel-containing catalysts for ethylene dimerization [1–7]. One of the remarkable features of this catalyst system is its activity in relation to a series of *n*-olefins. In contrast to the usual acid-type catalysts, the nickel oxide on silica or silica–alumina shows a higher activity for a lower alkene dimerization, particularly for ethylene [1,2]. The catalyst is also active for the isomerization of *n*-butenes, the mechanism of which has been proved to be of a proton donor–acceptor type [8]. It has been reported that the dimerization activities of such catalysts are related to the acidic properties of the surface and low-valent nickel ions [9]. In fact nickel oxide, which is active for $C_2H_4$–$C_2D_4$ equilibration, acquires an activity for ethylene dimerization upon addition of nickel sulfate, which is known to be an acid [10]. In the previous papers from our laboratory, it has been shown that NiO–$TiO_2$ and NiO–$ZrO_2$ modified with sulfate or tungstate ion are very active for ethylene dimerization [9,11–13]. High catalytic activities in the reaction were attributed to the enhanced acidic properties of the modified catalysts, which originated from the inductive effect of S=O or W=O bonds of the complex formed by the interaction of oxides with sulfate or tungstate ion. As an extension of the study on the ethylene dimerization, we have synthesized new catalysts of $NiSO_4/SiO_2$–$Al_2O_3$ which is active for ethylene dimerization even at room temperature, and the correlation between their acidic properties and catalytic activity for ethylene dimerization was studied.

## 2. Experimental

### 2.1. *Catalyst preparation*

The catalysts were prepared by the impregnation method using an aqueous solution of nickel sulfate. Silica–alumina having 66 wt% silica contents were obtained from Nikki Chemical Co., Japan. Silica gel was obtained from Davison Speciality Chemical Co., Baltimore, Maryland. Silica–alumina or silica gel was impregnated with an aqueous solution of $NiSO_4{\cdot}6H_2O$ followed by evaporating water, drying, and calcining in air at 300–800 °C for 1.5 h. It was used as catalyst after evacuation at different temperatures for 1 h. These series of catalysts are denoted by the weight percentage of $NiSO_4$. For example, 15-$NiSO_4/SiO_2$–$Al_2O_3$ or 15-$NiSO_4/SiO_2$ means the catalyst having 15 wt% of $NiSO_4$ using silica–alumina of 66 wt% silica or silica.

### 2.2. *Procedure*

Chemisorption of ammonia was employed as a measure of acidity of catalysts. The amount of chemisorption was obtained as the irreversible adsorption of ammonia [6,8]. Thus the first adsorption of ammonia at 20 °C and 300 Torr was followed by evacuation at 230 °C for 1 h and readsorption at 20 °C, the difference between two adsorptions at 20 °C giving the amount of chemisorption. An $NH_3$ temperature-programmed

---

[*] To whom correspondence should be addressed.

desorption (TPD) experiment was carried out using a flow system equipped with a thermal conductivity detector (TCD). Before experiment, the sample was pretreated at 500 °C for 1 h in He. Then it was cooled down and $NH_3$ was adsorbed at 100 °C. After removal of the weakly adsorbed $NH_3$ with purging in He, the sample was heated again from 100 to 800 °C at a heating rate of 10 °C/min in He flow, and held at 800 °C for 30 min. The Fourier transform infrared (FTIR) spectra were obtained in a heatable cell at room temperature using a Mattson Model GL6030E spectrometer. The self-supporting catalyst wafers contained about 9 mg/$cm^2$. Prior to obtaining the spectra the samples were heated under vacuum at 20–500 °C for 1 h.

The catalytic activity for ethylene dimerization was determined at 20 °C by a conventional static system by monitoring pressure decrease from an initial pressure of 300 Torr. A fresh catalyst sample of 0.2 g was used for every run and the catalytic activity was calculated as the amount of ethylene consumed in the initial 5 min. Reaction products were analyzed by gas chromatography with a VZ-7 column at room temperature.

## 3. Results and discussion

### 3.1. IR spectra and XRD

IR spectra of self-supported 15-$Ni(SO_4)_2/SiO_2$–$Al_2O_3$ after evacuation at 100–600 °C for 1 h are shown in figure 1. In general, for the metal oxides modified with sulfate ion followed by evacuating above 400 °C, a strong band assigned to S=O stretching frequency is observed at 1380–1370 $cm^{-1}$ [14–16]. In this work, the corresponding band for sample evacuated at 100 °C was not found because water molecules in the air were adsorbed on the surfaces of catalysts. These results are very similar to those reported by other authors [14–16]. The band at 1628 $cm^{-1}$ after evacuation at 100 °C is due to water molecules adsorbed on the surfaces of catalysts. However, from 200 °C the band appeared at 1370 $cm^{-1}$ as a shoulder, the band intensity increased with the evacuation temperature up to 500 °C, and the position of band shifted to a higher wavenumber (1391 $cm^{-1}$). That is, the higher the evacuation temperature, the larger the shift of the asymmetric stretching frequency of the S=O bonds. It is likely that the surface sulfur complexes formed by the interaction of oxides with sulfate ions in highly active catalysts have a strong tendency to reduce their bond order by the adsorption of basic molecules such as $H_2O$ [16,17]. Consequently, as shown in figure 1, an asymmetric stretching band of S=O bonds for the sample evacuated at lower temperature appears at a lower frequency compared with that for the sample evacuated at higher temperature because the adsorbed water reduces the bond order of S=O from a highly covalent double-bond character to a lesser double-bond character.

The XRD patterns of $NiSO_4/SiO_2$–$Al_2O_3$ containing different nickel sulfate contents and calcined at 500 °C for 1.5 h are shown in figure 2. The support, $SiO_2$–$Al_2O_3$ was amorphous to X-ray diffraction. For 10-$NiSO_4$/$SiO_2$–$Al_2O_3$ and 15-$NiSO_4/SiO_2$–$Al_2O_3$, no crystalline phase of nickel sulfate was observed, indicating that most of the nickel sulfate is present as amorphous $SiO_2$–$Al_2O_3$ due to the interaction between them [18]. However, as shown in figure 2, for $NiSO_4/SiO_2$–$Al_2O_3$ samples equal to or above 20%, an orthorhombic phase of $NiSO_4$ was

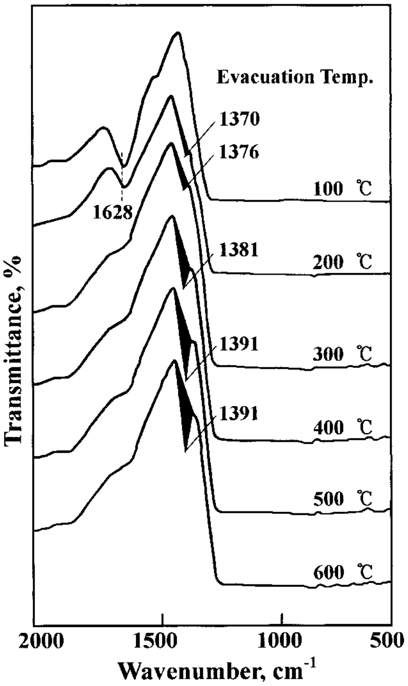

Figure 1. Infrared spectra of 15-$NiSO_4/SiO_2$–$Al_2O_3$ evacuated at different temperatures.

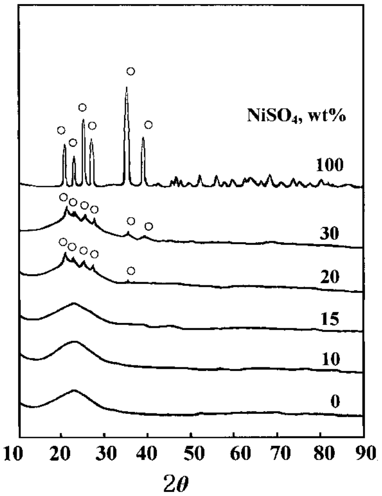

Figure 2. X-ray diffraction patterns of $NiSO_4/SiO_2$–$Al_2O_3$ having different $NiSO_4$ contents and calcined at 500 °C. ○, orthorhombic phase of $NiSO_4$.

Table 1
Specific surface area and acidity of $NiSO_4/SiO_2$–$Al_2O_3$ calcined at 500 °C for 1.5 h and 15-$NiSO_4/SiO_2$–$Al_2O_3$ calcined at various temperatures

| Weight % of $NiSO_4$ | Acidity ($\mu$mol/g)[a] | Surface area ($m^2$/g) |
|---|---|---|
| 0 | 105 (0.29) | 360 |
| 5 | 305 (0.87) | 352 |
| 10 | 338 (0.99) | 342 |
| 15 | 374 (1.28) | 292 |
| 20 | 352 (1.21) | 290 |
| 30 | 344 (1.46) | 236 |
| 40 | 301 (1.67) | 180 |
| 100 | 79 (2.63) | 30 |

| Calcination temperature of 15-$NiSO_4/SiO_2$–$Al_2O_3$ (°C) | Acidity ($\mu$mol/g)[a] | Surface area ($m^2$/g) |
|---|---|---|
| 300 | 331 (1.03) | 322 |
| 400 | 344 (1.08) | 318 |
| 450 | 347 (1.10) | 317 |
| 500 | 374 (1.28) | 292 |
| 550 | 355 (1.21) | 293 |
| 600 | 329 (1.13) | 290 |
| 700 | 212 (0.76) | 280 |
| 800 | 102 (0.41) | 252 |

[a] Acidity of $\mu$mol/$m^2$ unit given in parentheses.

observed. Therefore, it is assumed from the XRD results that the content of $NiSO_4$ forming a complete monolayer on the surface of $SiO_2$–$Al_2O_3$ is 15%.

### 3.2. Surface properties

It is necessary to examine the effect of nickel sulfate on the surface properties of catalysts, that is, specific surface area, acidity and acid strength. The specific surface areas of samples calcined at 500 °C and those of 15-$NiSO_4$/$SiO_2$–$Al_2O_3$ calcined at different temperatures for 1.5 h are listed in table 1. The presence of nickel sulfate strongly influences the surface area in comparison with the $SiO_2$–$Al_2O_3$. Specific surface areas of $NiSO_4/SiO_2$–$Al_2O_3$ samples decrease gradually with increasing nickel sulfate content and calcination temperature.

The acidity of catalysts calcined at 500 °C, as determined by the amount of $NH_3$ irreversibly adsorbed at 230 °C [18–20], is listed in table 1. The acidity increases abruptly upon the addition of nickel sulfate (5 wt% of $NiSO_4$) to $SiO_2$–$Al_2O_3$, and then the acidity increases very gently with increasing nickel sulfate content up to 15 wt% of $NiSO_4$. The acidity of 15-$NiSO_4/SiO_2$–$Al_2O_3$ increases with increasing calcination temperature, reaching a maximum at 500 °C, and then the acidity decreases with increasing calcination temperature. It is clear that the acidity of 15-$NiSO_4/SiO_2$–$Al_2O_3$ after 500 °C runs parallel with the surface area, as listed in table 1.

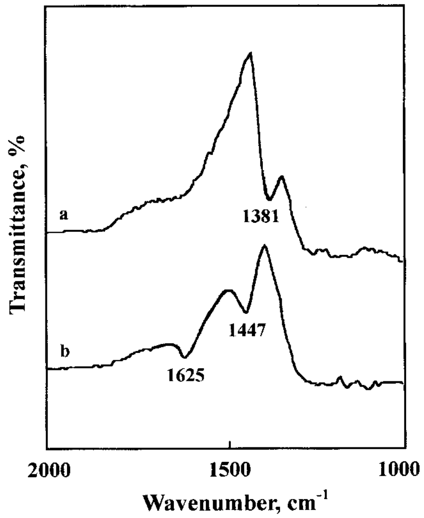

Figure 3. Infrared spectra of $NH_3$ adsorbed on 15-$NiSO_4/SiO_2$–$Al_2O_3$. (a) Background of 15-$NiSO_4/SiO_2$–$Al_2O_3$ after evacuation at 400 °C for 1 h, (b) $NH_3$ adsorbed on (a), where gas phase was evacuated at 230 °C for 1 h.

Infrared spectroscopic studies of ammonia adsorbed on solid surfaces have made it possible to distinguish between Brønsted and Lewis acid sites [21,22]. Figure 3 shows the IR spectra of ammonia adsorbed on 15-$NiSO_4/SiO_2$–$Al_2O_3$ samples evacuated at 400 °C for 1 h. For 15-$NiSO_4/SiO_2$–$Al_2O_3$ the band at 1447 $cm^{-1}$ is the characteristic peak of ammonium ion, which is formed on the Brønsted acid sites, and the absorption peak at 1625 $cm^{-1}$ is contributed by ammonia coordinately bonded to Lewis acid sites [21,22], indicating the presence of both Brønsted and Lewis acid sites on the surface of the 15-$NiSO_4/SiO_2$–$Al_2O_3$ sample. Other samples having different titanium sulfate contents also showed the presence of both Lewis and Brønsted acids. The intense band at 1381 $cm^{-1}$ after evacuation at 400 °C is assigned to the asymmetric stretching vibration of S=O bonds having a high double-bond nature [16,23]. However, the drastic shift of the IR band from 1381 $cm^{-1}$ to lower wavenumber (not shown due to the overlaps of skeletal vibration bands of $SiO_2$–$Al_2O_3$) after ammonia adsorption (figure 3(b)) indicates a strong interaction between an adsorbed ammonia molecule and the surface complex. Namely, the surface sulfur compound in the highly acidic catalysts has a strong tendency to reduce the bond order of SO from a highly covalent double-bond character to a lesser double-bond character when a basic ammonia molecule is adsorbed on the catalysts [16,17].

Acid stronger than $H_0 \leq -11.93$, which corresponds to the acid strength of 100% $H_2SO_4$, are superacids [24–27]. The strong ability of the sulfur complex to accommodate electrons from a basic molecule such as ammonia is a driving force to generate superacidic properties [16,23]. The 1390–1370 bands representing the asymmetric stretching of S=O are often regarded as the characteristic band of sulfated superacids [17,27].

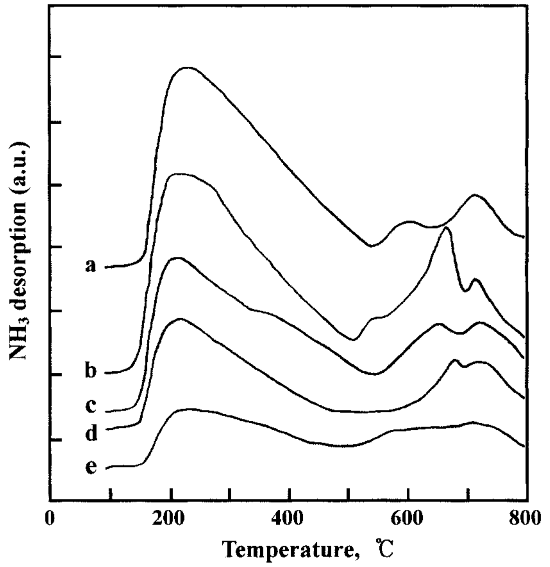

Figure 4. Temperature-programmed desorption profiles of ammonia from (a) 20-$NiSO_4/SiO_2$–$Al_2O_3$, (b) 15-$NiSO_4/SiO_2$–$Al_2O_3$, (c) 10-$NiSO_4/SiO_2$–$Al_2O_3$, (d) 5-$NiSO_4/SiO_2$–$Al_2O_3$ and (e) $SiO_2$–$Al_2O_3$.

As shown in figure 1, the asymmetric stretching bands of S=O after evacuation at 200–600 °C appeared at 1370–1391 $cm^{-1}$ differently depending on the evacuation temperature. The acid strength of $NiSO_4/SiO_2$–$Al_2O_3$ samples after evacuation at 500 °C for 1 h was also examined by a color-change method, using a Hammett indicator [13,28] in sulfuryl chloride. The samples were estimated to have $H_0 \leq -14.5$, indicating the formation of strong acidic sites. Consequently, $NiSO_4/SiO_2$–$Al_2O_3$ catalysts would be solid superacids, in analogy with the case of $ZrO_2$ modified with sulfate group [19,20,29].

### 3.3. TPD spectra of $NH_3$

The acid strength of the samples was examined by TPD curves of ammonia adsorbed on catalysts calcined at 500 °C as a function of temperature. As seen in figure 4, each curve displays a very broad peak, which is indicative of site heterogeneity. Although $SiO_2$–$Al_2O_3$ showed a little acidity, the acidity increased upon the addition of nickel sulfate to $SiO_2$–$Al_2O_3$, reaching a maximum at 15 wt% of $NiSO_4$, in agreement with those of figure 6 and table 1. For all samples, two regions below and above 500 °C appeared on the $NH_3$ TPD curve. The TPD curve below 500 °C was attributed to the desorption of $NH_3$ bound to Brønsted and Lewis acid sites. In fact, the existence of both Brønsted and Lewis acid sites was shown by the IR spectra of ammonia adsorbed on 15-$NiSO_4/SiO_2$–$Al_2O_3$ evacuated at 400 °C for 1 h. The high-temperature peaks of ammonia above 500 °C were ascribed to desorption of ammonia bound to strong Lewis acid sites. According to the previous report [25], Brønsted and Lewis acidity appears when the nickel sulfate is heat-treated below 500 °C, while that of Lewis acidity appears at higher temperatures.

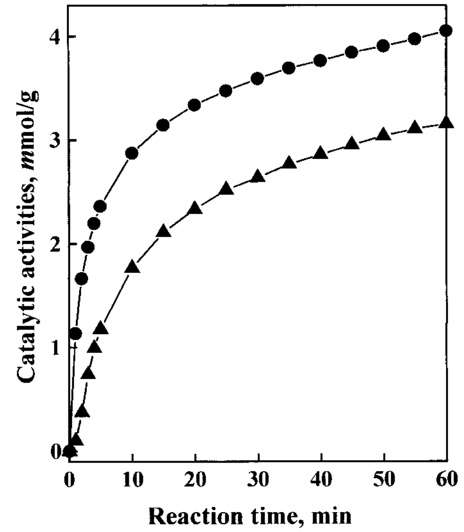

Figure 5. Time-course of ethylene dimerization over catalysts: ●, 15-$NiSO_4/SiO_2$–$Al_2O_3$, ▲, 5-$NiSO_4/SiO_2$–$Al_2O_3$.

Barthos *et al.* [30] also reported that for sulfated zirconia and sulfated zirconia–titania the strongest acid sites released $NH_3$ at temperatures as high as about 627 °C and these sites were shown to be of Lewis acid nature. The acid strength of $NiSO_4/SiO_2$–$Al_2O_3$ is exclusively higher than that of $SiO_2$–$Al_2O_3$, accounting for its high catalytic activity for ethylene dimerization. Especially, 15-$NiSO_4/SiO_2$–$Al_2O_3$ exhibited the highest acidity in this high-temperature region, explaining its highest catalytic activity for ethylene dimerization.

### 3.4. Ethylene dimerization over $NiSO_4/SiO_2$–$Al_2O_3$

$NiSO_4/SiO_2$–$Al_2O_3$ catalysts were tested for their effectiveness in ethylene dimerization. It was found that, over 5-$NiSO_4/SiO_2$–$Al_2O_3$ and 15-$NiSO_4/SiO_2$–$Al_2O_3$, ethylene was continuously consumed, as shown by the results presented in figure 5, where catalysts were evacuated at 500 °C for 1.5 h. Over $NiSO_4/SiO_2$–$Al_2O_3$, ethylene was selectively dimerized to *n*-butenes. However, a small amount of hexenes from the phase adsorbed on the catalyst surface was detected. The maximum conversion of ethylene over 15-$NiSO_4/SiO_2$–$Al_2O_3$ after 1 h was found to be 60%. In the composition of *n*-butenes analyzed by gas chromatography, 1-butene was found to predominate exclusively at the initial reaction time, as compared with *cis*-butene and *trans*-butene. However, the amount of 1-butene decreases with the reaction time, while the amount of 2-butene increases. Therefore, it seems likely that the initially produced 1-butene is also isomerized to 2-butene during the reaction time [11,13,29].

### 3.5. Correlation between acidity and catalytic activity

The catalytic activities of $NiSO_4/SiO_2$–$Al_2O_3$ and $NiSO_4/SiO_2$ for the reaction of ethylene dimerization

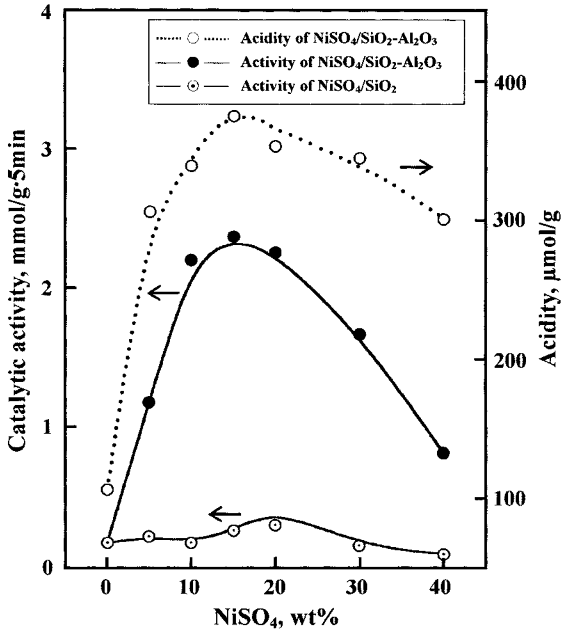

Figure 6. Catalytic activity for ethylene dimerization and acidity of $NiSO_4$/$SiO_2$–$Al_2O_3$ *versus* $NiSO_4$ content.

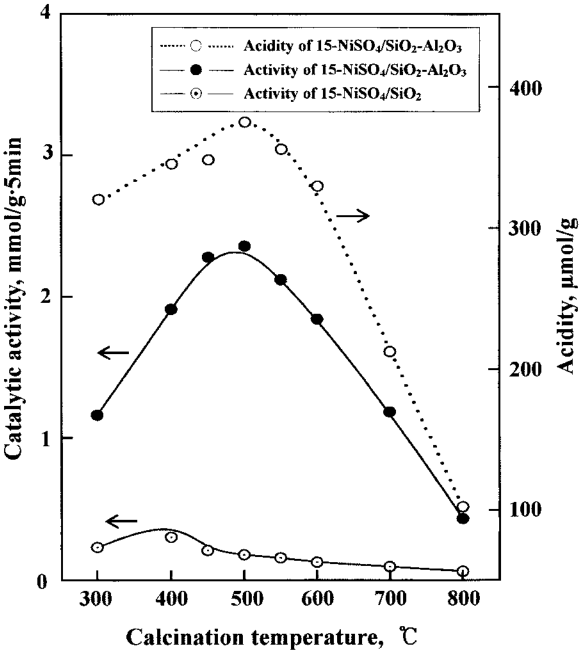

Figure 7. Catalytic activity for ethylene dimerization and acidity of 15-$NiSO_4$/$SiO_2$–$Al_2O_3$ *versus* calcination temperature.

were examined and the results are shown as a function of $NiSO_4$ content in figure 6, where the catalysts were evacuated at 500 °C for 1 h before reaction and the acidity of the catalyst is also given. The catalytic activities of $NiSO_4$/$SiO_2$–$Al_2O_3$ are very high compared with those of $NiSO_4$/$SiO_2$. Hereafter, emphasis is placed only on the $NiSO_4$/$SiO_2$–$Al_2O_3$. It is confirmed that the catalytic activities for $NiSO_4$/$SiO_2$–$Al_2O_3$ give a maximum at 15 wt% of $NiSO_4$. This is due to the increase of acidity by adding $NiSO_4$ to $SiO_2$–$Al_2O_3$. Comparing figure 6 and table 1, catalytic activity is closely correlated to the acidity of catalysts. That is, the higher the acidity, the higher the catalytic activity. Good correlations have been found in many cases between the acidity and the catalytic activities of solid acids. For example, the rates of both the catalytic decomposition of cumene and the polymerization of propylene over $SiO_2$–$Al_2O_3$ catalysts were found to increase with increasing acid amounts at strength $H_0 \leq +3.3$ [31]. It was also reported that the catalytic activity of nickel silicates in the ethylene dimerization as well as in the butene isomerization was closely correlated with the acidity of the catalyst [1]. As listed in table 1, the acidity attained a maximum when the $NiSO_4$ content in the catalyst was 15 wt%. However, the BET surface area decreases with an increasing nickel sulfate content, because nickel sulfate blocks the pore of $SiO_2$–$Al_2O_3$. It is known that acidity is required for the ethylene dimerization [1] and $SiO_2$–$Al_2O_3$ is a typical solid acid [31]. However, the $SiO_2$–$Al_2O_3$ without $NiSO_4$ was inactive as catalyst for ethylene dimerization, but the $NiSO_4$/$SiO_2$–$Al_2O_3$ exhibited high catalytic activity even at room temperature.

The effect of calcination temperature on the catalytic activities of 15-$NiSO_4$/$SiO_2$–$Al_2O_3$ and 15-$NiSO_4$/$SiO_2$ was also examined, where the catalysts were calcined for 1 h. As shown in figure 7, the maximum activity is obtained with the catalyst calcined at 500 °C. The maximum activity at a calcination temperature of 500 °C can be explained in terms of the maximum acidity at 500 °C. The acidity of 15-$NiSO_4$/$SiO_2$–$Al_2O_3$ calcined at various temperatures is listed in table 1. Comparing table 1 and figure 7, catalytic activity as a function of calcination temperature is also correlated to the acidity of catalysts. With 15-$NiSO_4$/$SiO_2$ the catalytic activity is also very low at all calcination temperatures.

### 3.6. Active sites

$SiO_2$–$Al_2O_3$ alone without $NiSO_4$ was totally inactive for the dimerization reaction at room temperature. The catalyst calcined at 900 °C, which has no sulfate ion due to the complete decomposition, was also inactive for dimerization. Therefore, it is believed that the active site responsible for dimerization consists of a low-valent nickel and an acid, as observed in the NiO-containing catalysts [9,13,32]. The term "low-valent nickel" originated from the fact that the NiO-$SiO_2$ catalyst was drastically poisoned by carbon monoxide, since a low-valent nickel is prone to chemisorb carbon monoxide [32]. In this work, all catalysts added with $NiSO_4$ were poisoned by 1 $\mu$mol $g^{-1}$ of carbon monoxide for dimerization. It seems that the formation of low-valent nickel is caused by evacuation at high temperature.

The IR spectra of CO adsorbed on 15-$NiSO_4$/$SiO_2$–$Al_2O_3$ were examined to clarify the formation of

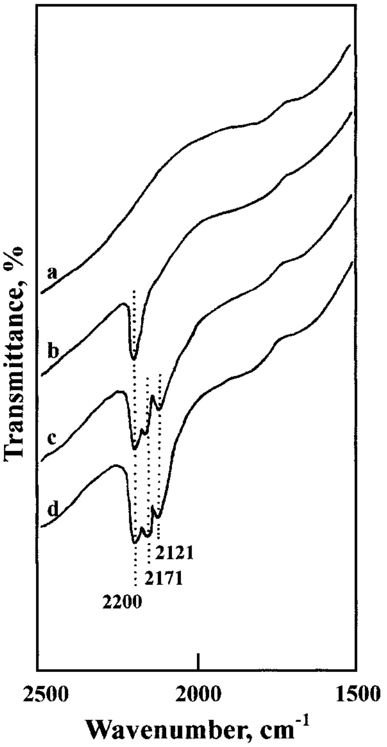

Figure 8. The infrared spectra of CO adsorbed on 15-$NiSO_4/SiO_2$–$Al_2O_3$. (a) Background of 15-$NiSO_4/SiO_2$–$Al_2O_3$ evacuated at room temperature, (b) after the introduction of 40 Torr CO to sample (a), (c) after the introduction of 90 Torr CO to the sample evacuated at 500 °C for 1 h and (d) after the introduction of 140 Torr CO to the sample (c).

low-valent nickel. When the sample was exposed to CO (40 Torr) at room temperature, the adsorbed CO band appeared at 2200 cm$^{-1}$, as shown in figure 8(b). The band might be assigned to the stretching vibration for CO adsorbed on $Ni^{2+}$ [33,34]. However, when the sample evacuated at 500 °C for 1 h was exposed to CO (90 Torr), the two bands at 2171 and 2121 cm$^{-1}$, in addition to the band at 2200 cm$^{-1}$, were observed (figure 8(c)). The intensities of two bands increased concomitantly with increasing CO concentration, as shown in figure 8d. Therefore, it seems likely that the two bands originate from one species, $Ni^+(CO)_2$. The bands at 2171 and 2121 cm$^{-1}$ are assigned to symmetrical and asymmetrical stretching vibrations of $Ni^+(CO)_2$, respectively [33,34]. In view of IR results of adsorbed CO, it is concluded that the active sites responsible for ethylene dimerization consist of a valent nickel, $Ni^+$, and an acid.

## 4. Conclusions

A series of catalysts, $NiSO_4/SiO_2$–$Al_2O_3$, for ethylene dimerization were prepared by the impregnation method using an aqueous solution of nickel sulfate. Although $SiO_2$–$Al_2O_3$ without $NiSO_4$ was totally inactive for ethylene dimerization, the $NiSO_4$ supported on $SiO_2$–$Al_2O_3$ exhibited high catalytic activity even at room temperature. The high catalytic activity of $NiSO_4$/$SiO_2$–$Al_2O_3$ was closely correlated with the increase of acidity and acid strength due to the addition of $NiSO_4$. In view of IR results of adsorbed CO, it is confirmed that the active sites responsible for ethylene dimerization consist of a low-valent nickel, $Ni^+$, and an acid.

## Acknowledgment

This work was supported by grant 2001-1-30700-006-2 from the Basic Research Program of the Korea Science Engineering Foundation.

## References

[1] J.R.Sohn and A. Ozaki, J. Catal. 61 (1980) 29.
[2] G. Wendt, D. Hentschel, J. Finster and R. Schöllner, J. Chem. Soc., Faraday Trans. I, 79 (1983) 2013.
[3] K. Urabe, M. Koga and Y. Izumi, J. Chem. Soc., Chem. Commun. (1989) 807.
[4] L. Bonneviot, D. Olivier and M. Che, J. Mol. Catal. 21 (1983) 415.
[5] M. Hartmann, A. Pöppl and L. Kevan, J. Phys. Chem. 100 (1996) 9906.
[6] F. Bernardi, A. Bottoni and I. Rossi, J. Am. Chem. Soc. 120 (1998) 7770.
[7] H. Choo and L. Kevan, J. Phys. Chem. B 105 (2001) 6353.
[8] A. Ozaki and K. Kimura, J. Catal. 3 (1964) 395.
[9] J.R. Sohn and D.C. Shin, J. Catal. 160 (1996) 314.
[10] K. Maruya and A. Ozaki, Bull. Chem. Soc. Jpn. 46 (1973) 351.
[11] J.R. Sohn and H.J. Kim, J. Catal. 101 (1986) 428.
[12] J.R. Sohn, H.W. Kim and J.T. Kim, Korean J. Chem. Eng. 4 (1987) 1.
[13] J.R. Sohn, and S.Y. Lee, Appl. Catal. A: General 164 (1997) 127.
[14] O. Saur, M. Bensitel, A.B.H. Saad, J.C. Lavalley, C.P. Tripp and B.A. Morrow, J. Catal. 99 (1986) 104.
[15] B.A. Morrow, R.A. McFarlane, M. Lion and J.C. Lavalley, J. Catal. 107 (1987) 232.
[16] T. Yamaguchi, Appl. Catal. 61 (1990) 1.
[17] T. Jin, T. Yamaguchi and K. Tanabe, J. Phys. Chem. 90 (1986) 4794.
[18] J.R. Sohn, S.G. Cho, Y.I. Pae and S. Hayashi, J. Catal. 159 (1996) 170.
[19] J.R. Sohn and E.H. Park, J. Ind. Eng. Chem. 4 (1998) 197.
[20] J.R. Sohn and M.Y. Park, J. Ind. Eng. Chem. 4 (1998) 84.
[21] J.R. Sohn and E.H. Park, J. Ind. Eng. Chem. 6 (2000) 312.
[22] A. Satauma, A. Hattori, K. Mizutani, A. Furuta, A. Miyamoto, T. Hattori and Y. Murakami, J. Phys. Chem. 92 (1988) 6052.
[23] J.R. Sohn, E.H. Park and H.W. Kim, J. Ind. Eng. Chem. 5 (1999) 253.
[24] T.K. Cheung, J.L. d'Itri, F.C. Lange and B.C. Gates, Catal. Lett. 31 (1995) 153.
[25] K. Tanabe, M. Misono, Y. Ono and H. Hattori, *New Solid Acids and Bases* (Elsevier Science: Amsterdam, 1989) ch. 4.
[26] K. Arata, Adv. Catal. 37 (1990) 165.
[27] F.G.A. Olah, G.K.S. Prakash and J. Sommer, Science 206 (1979) 13.
[28] J.R. Sohn and S.G. Ryu, Langmuir 9 (1993) 126.
[29] J.R. Sohn, H.W. Kim, M.Y. Park, E.H. Park, J.T. Kim and S.E. Park, Appl. Catal. A: General 128 (1995) 127.
[30] R. Barthos, F. Lónyi, Gy. Onyestyák and J. Valyon, J. Phys. Chem. B 104 (2000) 7311.
[31] K. Tanabe, *Solid Acids and Bases* (Kodansha, Tokyo, 1970).
[32] K. Kimura, H.A.-I and A. Ozaki, J. Catal. 18 (1970) 271.
[33] M. Kermarce, D. Oliver, M. Richard, M. Che and F. Bozon-Verduraz, J. Phys. Chem. 86 (1982) 2818.
[34] P.H. Kasai, R.J. Bishop Jr. and D. McLeod Jr., J. Phys. Chem. 82 (1978) 279.